Supporting Information

MoC_xN_y Heterostructure Derived from Polyoxometalate Hybrid for Hydrogen Transfer Cascade Coupling of Nitroarenes and Alcohols

Zhe Wang,[a] Wenrui Zhao,[a] Zhouyang Long,[b] Tengfei Niu,[a] Pingbo Zhang,[a] Mingming Fan,[a] Yan Leng*[a]

[a] Key Laboratory of Synthetic and Biological Colloids, Ministry of Education, School of Chemical and Material Engineering, Jiangnan University, Wuxi 214122 (China)

E-mail: yanleng@jiangnan.edu.cn

[b] Jiangsu Key Laboratory of Green Synthetic Chemistry for Functional Materials, School of Chemistry & Materials Science, Jiangsu Normal University, Xuzhou 221116 (China)

E-mail: longzhouyangfat@163.com

Table of Content

Experimental Section

Materials

L-histidine ($C_6H_9N_3O_2$), n-hexane (C_6H_{14}), potassium t-butoxide (C_4H_9OK), silicic acid (H_2SiO_3), and nitrobenzene ($C_6H_5NO_2$) were purchased from Aladdin Reagent Company. Phosphomolybdic acid ($H_3PMo_{12}O_{40}$), tannic acid ($C_{76}H_{52}O_{46}$), aniline (C_6H_7N), benzyl alcohol (C_7H_8O), benzaldehyde (C_7H_6O), 1,4-Dioxane ($C_4H_8O_2$), DMSO (C_2H_6OS), toluene (C_7H_8) and xylene (C_8H_{10}) were obtained from Sinopharm Chemical Reagent Co. Ltd. Ethanol (C_2H_6O) was purchased from Greagent Company. Deionized water was used, and all reagents did not need further purification.

Characterizations

The XRD information of the catalysts was acquired using a D8 X-advanced powder diffractometer of Bruker AXS, with tube current and tube voltage set at 40 mA and 40 kV, respectively, equipped with a solid-state detector and Cu Kα radiation, and scanned over the range of 5-90° at a rate of 5°/min, and the samples were characterized in terms of their crystallinity and crystalline phase. The surface chemical states of the samples were measured at a 12 kV, 12 mA Al Ka x-ray source (1486.6 eV). The binding energy was corrected using the C 1s peak (284.8 eV) as a reference to minimize the charge effect of the sample. The morphology of the catalyst was observed with the S-4800 field emission scanning electron microscope (SEM) of Hitachi. The TEM was done on a JEM-2100PLUS transmission electron microscope. The STEM was done on a FEI Talos F200X G2 transmission electron microscope. The samples were dissolved in anhydrous ethanol, and the mixture was sonicated for 5 min. Energy–dispersive X–ray spectroscopy (EDS) mapping was also combined for elemental analysis. Infrared spectra were obtained using an FT-IR instrument with a Nicolet iS50, and the wavelength range was chosen to be 4000-500 cm^{-1}. The catalyst porous structure parameters were determined by the Brunauer-Emmett-Teller (BET) method by N_2 adsorption-desorption isotherms using Micromeritics ASAP 2460 at 77K. The pore volume and pore size of the samples were calculated by the Barrett-Joyner-Halenda (BJH) method. The hydrogen overflow capacity of the calcined catalysts was tested (H_2-TPD) using a BELCAT-II programmed temperature rise desorption apparatus from Macchik Bayer, Japan. Hydrogen desorption measurements were made by heating the catalyst sample in 20 mL/min Ar, from 50°C to 800°C, with a temperature rate of 10°C/min.

DFT calculations

DFT calculations for cluster models were performed using Gaussian 09 program (version D.01).[1-3] Geometry optimization was conducted at the B3LYP/def2-SVP level of theory, which were dispersion corrected by D3BJ; the single point calculations for the optimized geometries were performed to obtain accurate energies at the M062x/def2-TZVP level of theory, which were dispersion corrected by D3.[4-7] Vibrational frequency analysis was carried out to identify the nature of each stationary points as a minimum or a transition state, and to acquire the Gibbs free energy correction. The solvent effect was evaluated by the SMD solvation model. The Gibbs free energies were included in the Gibbs energy correction of unscaled vibrational analysis at the B3LYP/def2-SVP (D3BJ) level of theory.

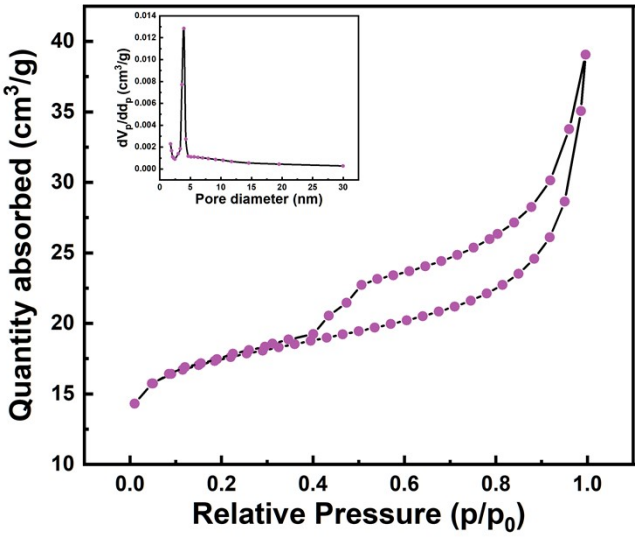

Figure S1. N_2 adsorption-desorption isotherms and pore-size distribution of MoC_xN_y@SiCN.

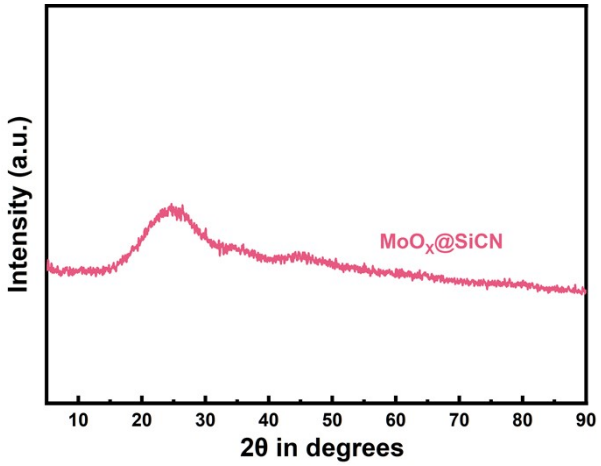

Figure S2. XRD spectrum of MoO_x@SiCN.

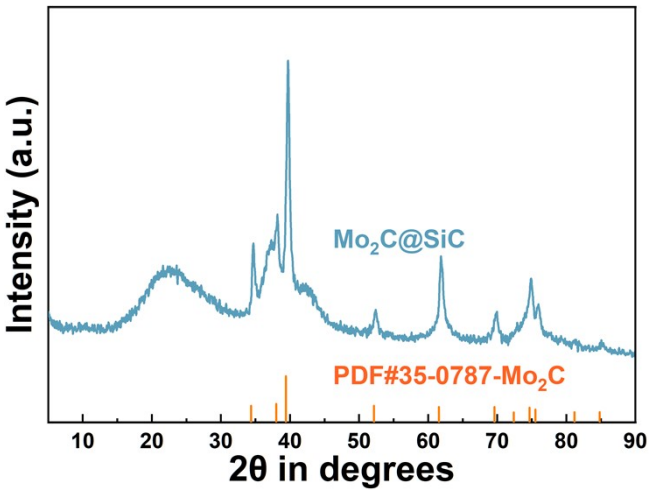

Figure S3. XRD spectrum of Mo_2C@SiC.

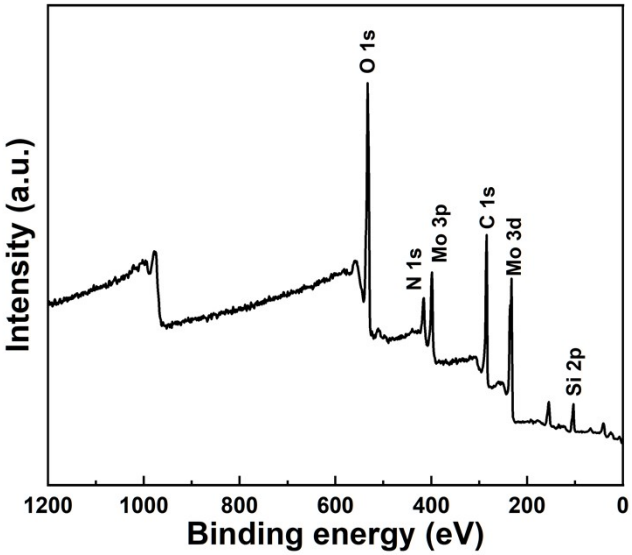

Figure S4. XPS spectrum of MoC_xN_y@SiCN.

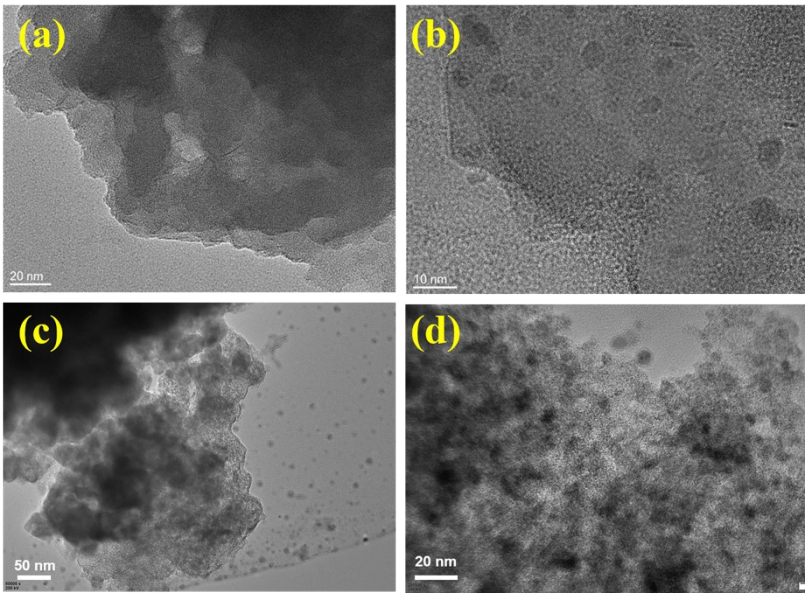

Figure S5. TEM images of MoC_xN_y@SiCN (a and b) and MoC_xN_y@CN (c and d).

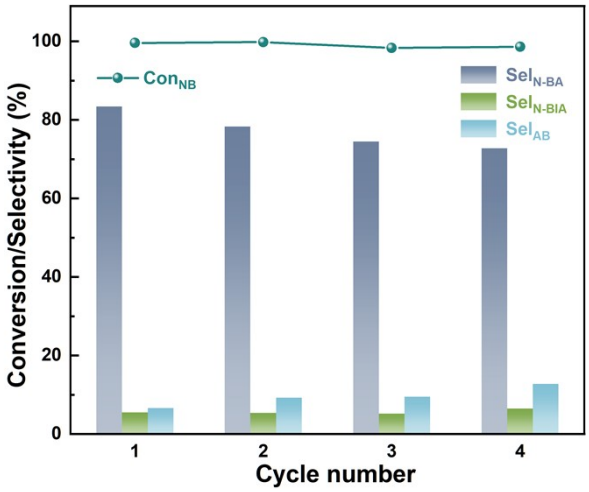

Figure S6. Reusability of MoC_xN_y@SiCN-catalyzed coupling of nitrobenzene and benzyl alcohol.

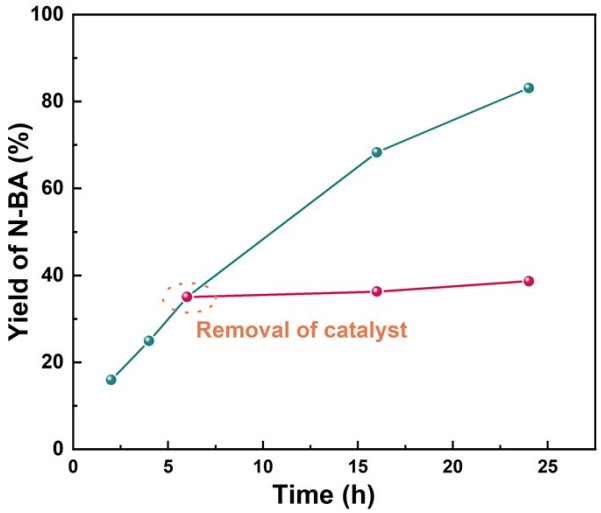

Figure S7. Hot-filtration experiment; The green and the pink lines indicate the represent the yield of N-BA without or after removal of the catalyst, respectively.

a: MoC_xN_y system

IM1	TS_{1-2}	IM2	IM3
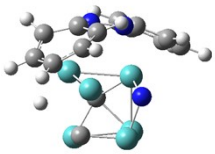	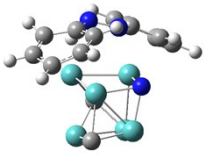	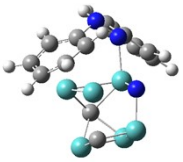	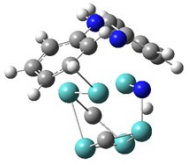
TS_{3-4}	IM4	IM5	TS_{5-6}
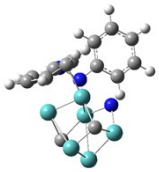	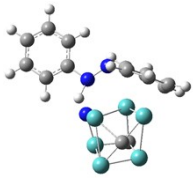	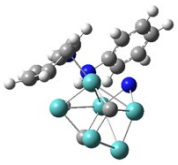	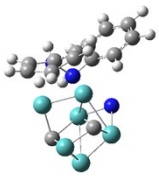
IM6	TS_{6-7}	IM7	TS_{7-8}
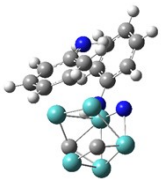	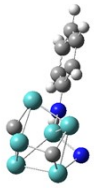	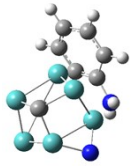	
IM8			
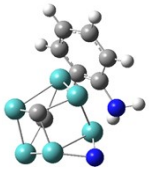			

Figure S8. The initial structure, transition state, and the final structure of azobenzene in n-hexane solvent being hydrogenated on MoC_xN_y to convert into aniline.

b: Mo_2C system

IM1	TS_{1-2}	IM2	IM3
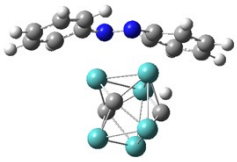	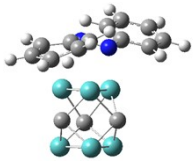	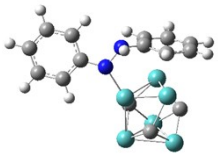	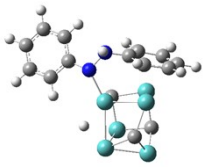
TS_{3-4}	IM4	IM5	TS_{5-6}
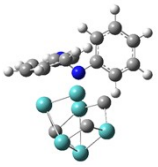	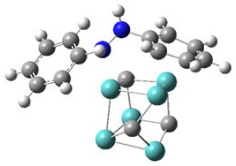	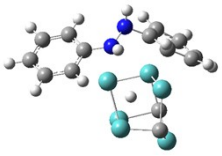	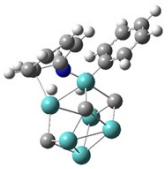
IM6	TS_{6-7}	IM7	TS_{7-8}
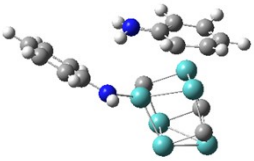	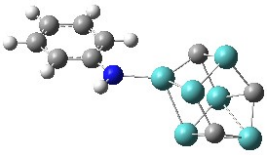	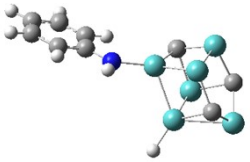	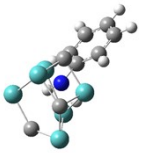
IM8			
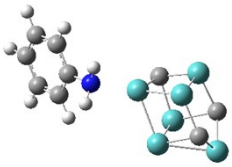			

Figure S9. The initial structure, transition state, and the final structure of azobenzene in n-hexane solvent being hydrogenated on Mo_2C to convert into aniline.

Table S1. Experimental optimization of solvent, base type, and base dosage.

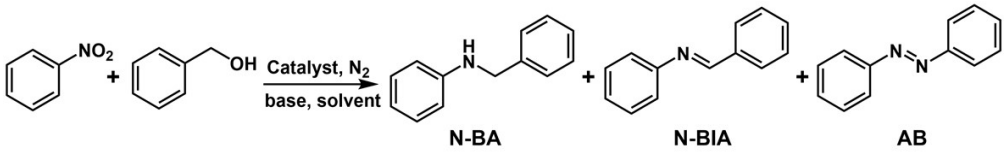

Entry	Solvent	Base (equiv)	Time (h)	T (℃)	Con (%)	Sel (%)		
						N-BA	N-BIA	AB
1	n-hexane	t-BuOK/2	24	150	100	82.8	5.0	4.2
2	n-hexane	t-BuOK/3	24	150	100	83.4	3.8	5.4
3	n-hexane	t-BuOK/4	24	150	99.8	87.4	3.7	2.8
4	DMSO	t-BuOK/2	24	150	100	47.1	1.9	43.9
5	toluene	t-BuOK/2	24	150	100	24.3	52.0	17.4
6	xylene	t-BuOK/2	24	150	100	0.2	46.3	48.6
7	1,4-Dioxane	t-BuOK/2	24	150	100	13.3	39.7	41.8
8	ethanol	t-BuOK/2	24	150	90.7	0.6	3.7	92.4
9	free	t-BuOK/2	24	150	99.1	12.2	2.8	73.2
10	n-hexane	free	24	150	9.6	11.1	55.7	33.0
11	n-hexane	t-BuOK/1	24	150	82.7	42.4	30.5	22.6
12	n-hexane	K_2CO_3/2	24	150	100	27.4	46.3	18.5
13	n-hexane	NaOH/2	24	150	100	8.4	55.8	32.4
14	n-hexane	KOH/2	24	150	99.6	0.9	32.2	60.1

Reaction conditions: nitrobenzene (0.5 mmol), benzyl alcohol (2 mmol), catalyst (20 mg), base, solvent (1 mL).

Table S2. Experimental optimization of the ratio of nitrobenzene to benzyl alcohol.

Entry	n(NB):n(BA)	Time (h)	T(℃)	Con (%)	Sel (%)		
					N-BA	N-BIA	AB
1	1:2	24	150	100	62.2	11.3	20.7
2	1:3	24	150	100	78.3	5.1	10.3
3	1:4	24	150	99.6	83.3	5.5	6.6
4	1:5	24	150	100	64.0	14.3	14.5
5	1:6	24	150	99.8	58.6	12.7	21.8
6	1:4	24	140	100	49.0	11.7	34.8
7	1:4	24	160	100	86.1	3.2	4.8
8	1:4	24	170	100	97.1	0.4	0.8

Reaction conditions: nitrobenzene (0.5 mmol), benzyl alcohol, catalyst (20 mg), base (t-BuOK, 2 equiv), n-hexane (1 mL), 24 h.

Table S3. Comparison of previous work on the coupling of nitrobenzene with benzyl alcohol to form N-benzylaniline.

Entry	Catalyst	Reaction conditions	Product	Yield (%)	Ref
1	Au/TiO_2-VS	1 mmol nitrobenzene, 8 mmol benzyl alcohol, 1 mL toluene, 0.5 mol % catalyst, 120°C, Ar, 14 h.	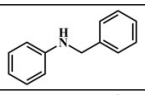	> 99	[8]
2	9.1 wt% Au/Fe_2O_3	5 mmol nitrobenzene, 50 mmol benzyl alcohol, 0.1 g catalyst, Ar, 160°C, 8 h.	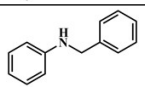	> 9	[9]
3	$RuCl_3$	1 mmol nitrobenzene, 1 mmol benzyl alcohol, 1.5 g glycerol, 0.5 mL TFMB, 2.5 mol % catalyst, 10% mmol ligand, 10 mol % K_2CO_3, 130°C, Ar, 24 h.	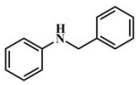	91	[10]
4	$Mo(CO)_3$	0.5 mmol nitrobenzene, 3 mmol benzyl alcohol, 1 mL n-hexane, 5 mol % catalyst, t-BuOK (5 equiv), 150°C, 24 h.	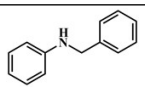	80	[11]
5	Ni-Al_2O_3-HFA	$n_{substrate}$ = 0.81mmol, 150 mg catalyst, 2 MPa H_2, 230°C, 400 min.	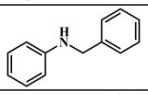	97	[12]
6	Iridium catalyst	1 mmol nitrobenzene, 5 mmol benzyl alcohol, 2 mL toluene, 1 mol % catalyst, t-BuOK (5 mmol), 100°C, 10 h.	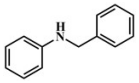	90	[13]
7	Ag-MCP-1	1 mmol nitrobenzene, 1 mmol benzyl alcohol, 1 g glycerol, 2 mL xylene, 25 mg catalyst, 10 mol % K_2CO_3, N_2, 150°C, 24 h.	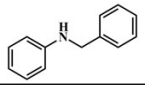	93	[14]
8	1% RuPd/TiO_2	4.5 mmol nitrobenzene, 4.5 mmol benzyl alcohol, 0.1 g catalyst, 5 mL mesitylene, 20 bar H_2, 160°C, 3 h.	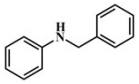	66	[15]
9	Ir^{III}/Au^{I}	0.3 mmol nitrobenzene, 1 mL benzyl alcohol, 0.5% catalyst, 0.3 mmol of Cs_2CO_3, 100°C, 22 h.	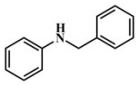	82	[16]
10	Co–N–C/CNT@AC	2 mmol nitrobenzene, 24 mmol benzyl alcohol, 240 mg catalyst, solvent-free, N_2, 160°C, 38 h.	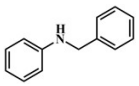	82	[17]
11	Ag/Al_2O_3	1 mmol nitrobenzene, 6 mmol benzyl alcohol, 2.2 mol % catalyst, 5 mL xylene, 100 mg Cs_2CO_3, N_2, 140°C, 20 h.	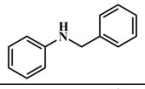	98	[18]
12	Au/Ag–Mo-NR	1 mmol nitrobenzene, 1 mmol benzyl alcohol, 0.5 mL xylene, 40 mg catalyst, 10 mol % K_2CO_3, 1 g glycerol, Ar, 150°C, 24 h.	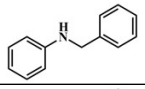	91	[19]
13	$Cu/Zr(OH)_4$	1 mmol nitrobenzene, 1 mmol benzyl alcohol, 110 mg catalyst, 10 mL n-octane, 180°C, 0.5 MPa H_2, 7 h.	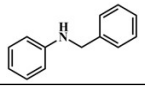	> 99	[20]
14	MoC_xN_y@SiCN	0.5 mmol nitrobenzene, 2 mmol benzyl alcohol, 1 mL n-hexane, 20 mg catalyst, 1 mmol t-BuOK, 150°C, 24 h.	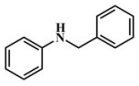	83	This work

Table S4. Effect of different hydrogen sources on the selectivity of N-alkylation of nitrobenzene with alkyl alcohol.

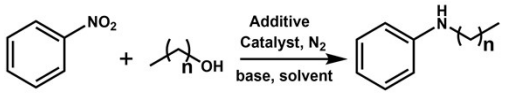

Entry	Catalyst	Additive	Product	Yield(%)
1	MoC_xN_y@SiCN	0.5 g glycerol	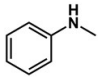	75.4
2	MoC_xN_y@SiCN	1.5 mmol HCOONa	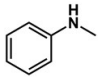	6.2
3	MoC_xN_y@SiCN	0.5 g glycerol	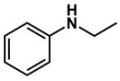	82.3
4	MoC_xN_y@SiCN	1.5 mmol HCOONa	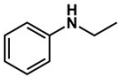	0.1
5	MoC_xN_y@SiCN	0.5 g glycerol	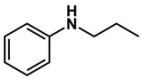	72.0
6	MoC_xN_y@SiCN	1.5 mmol HCOONa	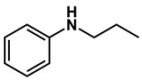	1.8
7	MoC_xN_y@SiCN	0.5 g glycerol	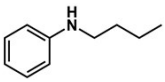	49.5
8	MoC_xN_y@SiCN	1.5 mmol HCOONa	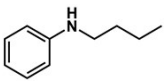	0.8
9	MoC_xN_y@SiCN	1.5 mmol HCOOH	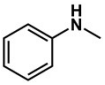	90.5
10	MoC_xN_y@SiCN	1.5 mmol HCOOH	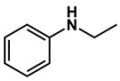	81.4
11	MoC_xN_y@SiCN	1.5 mmol HCOOH	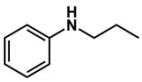	82.2
12	MoC_xN_y@SiCN	1.5 mmol HCOOH	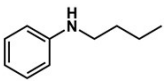	78.8

Reaction conditions: nitrobenzene (0.5 mmol), alkyl alcohol (2 mmol), catalyst (MoC_xN_y@SiCN, 20 mg), base (t-BuOK, 2 equiv), n-hexane (1 mL), 130℃, 24 h.

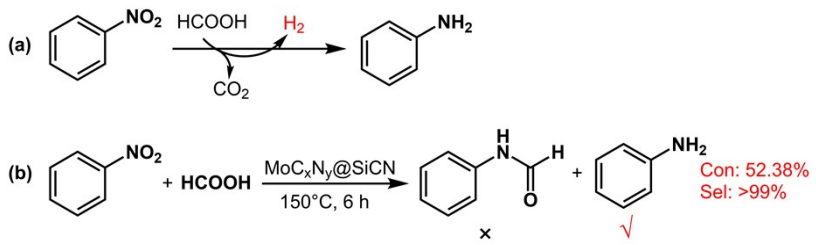

Scheme S1. Experiments on the reaction mechanism of nitrobenzene with formic acid.

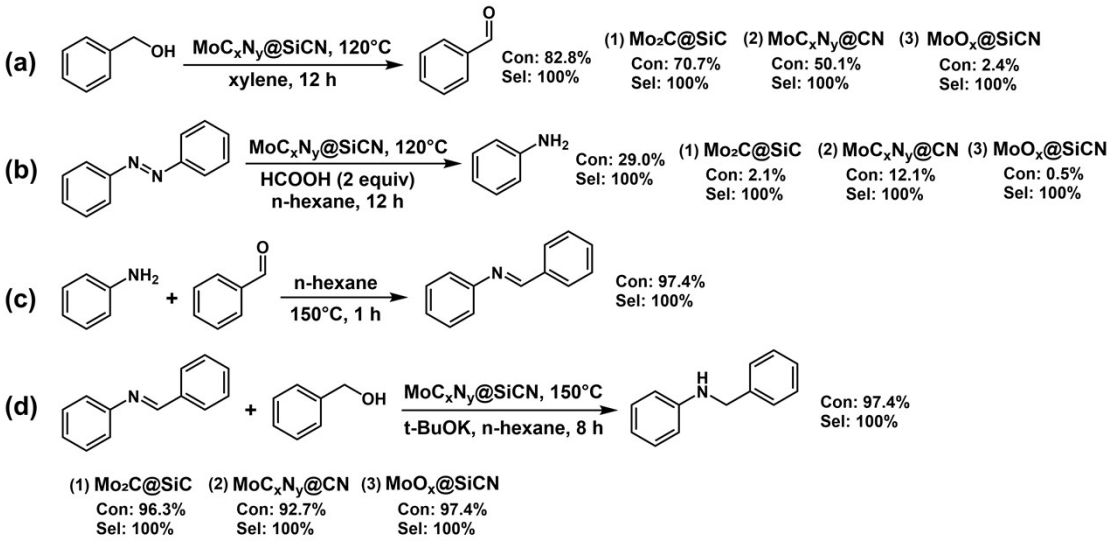

Scheme S2. (a) The dehydrogenation of benzyl alcohol. (b) Hydrogenation of azobenzene using formic acid as a hydrogen source. (c) The condensation reaction of benzaldehyde and aniline. (d) The hydrogenation of N-benzylideneaniline with benzyl alcohol as a hydrogen source.

References

1 W. J. Hehre, R. Ditchfield and J. A. Pople, *J. Chem. Phys.* 1972, **56**, 2257-2261.
2 R. Krishnan, J. S. Binkley, R. Seeger and J. A. Pople, *J. Chem. Phys.* 1980, **72**, 650-654.
3 M. Frisch, G. Trucks, H. Schlegel, G. Scuseria, M. Robb, J. Cheeseman, G. Scalmani, V. Barone, B. Mennucci and G. J. G. I. W. Petersson, CT, USA, 2013.
4 F. Weigend and R. Ahlrichs, *Phys. Chem. Chem. Phys.*, 2005, **7**, 3297-3305.
5 S. Grimme, J. Antony, S. Ehrlich and H. Krieg, *J. Chem. Phys.*, 2010, **132**, 154104.
6 S. Grimme, S. Ehrlich and L. Goerigk, *J. Comput. Chem.*, 2011, **32**, 1456-1465.
7 Y. Li, J. Carroll, B. Simpkins, D. Ravindranathan, C. M. Boyd and S. Huo, *Organometallics*, 2015, **34**, 3303-3313.
8 C. H. Tang, L. He, Y. M. Liu, Y. Cao, H. Y. He and K. N. Fan, *Chem.*, 2011, **17**, 7172-7177.
9 Q. Peng, Y. Zhang, F. Shi and Y. Deng, *Chem. Commun.*, 2011, **47**, 6476-6478.
10 X. Cui, Y. Deng and F. Shi, *ACS Catal.*, 2013, **3**, 808-811.
11 W. Li, M. Huang, J. Liu, Y.-L. Huang, X.-B. Lan, Z. Ye, C. Zhao, Y. Liu and Z. Ke, *ACS Catal.*, 2021, **11**, 10377-10382.
12 W. Li, J. Shi, D. He and H. Chen, *Inorg. Chem.*, 2023, **62**, 21470-21478.
13 Y. Wang, F. L. Zhang, Z. J. Liu and Z. J. Yao, *Inorg. Chem.*, 2022, **61**, 10310-10320.
14 U. Mandi, A. S. Roy, S. K. Kundu, S. Roy, A. Bhaumik and S. M. Islam, *J. Colloid Interface Sci.,* 2016, **472**, 202-209.
15 M. Sankar, Q. He, S. Dawson, E. Nowicka, L. Lu, P. C. A. Bruijnincx, A. M. Beale, C. J. Kiely and B. M. Weckhuysen, *Catal. Sci. Technol.,* 2016, **6**, 5473-5482.
16 M. Böhmer, F. Kampert, T. T. Y. Tan, G. Guisado-Barrios, E. Peris and F. E. Hahn, *Organometallics*, 2018, **37**, 4092-4099.
17 D. Liu, P. Yang, H. Zhang, M. Liu, W. Zhang, D. Xu and J. Gao, *Green Chem.*, 2019, **21**, 2129-2137.
18 H. Liu, G. K. Chuah and S. Jaenicke, *Phys. Chem. Chem. Phys.*, 2015, **17**, 15012-15018.
19 X. Cui, C. Zhang, F. Shi and Y. Deng, *Chem. Commun.*, 2012, **48**, 9391-9393.
20 J. Song, C. Che, Y. Dai, J. Qin, C. Yang, Z. Chen, K. Ma, Y. Han and Y. Long, *ACS Catal.*, 2025, **15**, 1170-1181.